Rai, A.C. and Chen, Q. 2012. "Simulations of ozone distributions in an aircraft cabin using computational fluid dynamics," *Atmospheric Environment,* 54, 348-357.

Simulations of Ozone Distributions in an Aircraft Cabin Using Computational Fluid Dynamics

Aakash C. Rai[1] and Qingyan Chen[1, 2*]
[1] School of Mechanical Engineering, Purdue University, West Lafayette, IN 47907, USA
[2] School of Environmental Science and Technology, Tianjin University, Tianjin 300072, China
[*]Phone: (765) 496-7562, FAX: (765) 496-0539, Email: yanchen@purdue.edu

Abstract

Ozone is a major pollutant of indoor air. Many studies have demonstrated the adverse health effect of ozone and the byproducts generated as a result of ozone-initiated reactive chemistry in an indoor environment. This study developed a Computational Fluid Dynamics (CFD) model to predict the ozone distribution in an aircraft cabin. The model was used to simulate the distribution of ozone in an aircraft cabin mockup for the following cases: (1) empty cabin; (2) cabin with seats; (3) cabin with soiled T-shirts; (4) occupied cabin with simple human geometry; and (5) occupied cabin with detailed human geometry. The agreement was generally good between the CFD results and the available experimental data. The ozone removal rate, deposition velocity, retention ratio, and breathing zone levels were well predicted in those cases. The CFD model predicted breathing zone ozone concentration to be 77-99% of the average cabin ozone concentration depending on the seat location. The ozone concentration at the breathing zone in the cabin environment can better assess the health risk to passengers and can be used to develop strategies for a healthier cabin environment.

Keywords: Ozone; Aircraft cabin; Air quality; CFD; Surface chemistry; Breathing zone

Nomenclature

A	area of the ozone deposition surface
C	ozone concentration
$C_{ambient}$, C_{BZ}, C_{cabin}, C_{inlet}, and C_{outlet}	ambient, breathing zone, volume averaged cabin, inlet, and outlet ozone concentrations
C_t	cabin ozone concentration at time t
C_μ	constant in the k-ε model (0.09)
D_o	binary diffusion coefficient of ozone in air
J_s	ozone deposition flux at surface
k	turbulent kinetic energy
l	mean molecular free path
L_{in}	turbulence length scale
m	mass of an individual ozone molecule
Q	supply airflow rate to the cabin
r_{ozone}	ozone ratio
S_c	ozone source
Sc_t	turbulent Schmidt number
t	time
T	air temperature in Kelvin
$\vec{u}$	air velocity vector
U_{in}	air velocity at inlet
v_d	ozone deposition velocity
v_t	transport limited deposition velocity
V_{cabin}	volume of the air inside the cabin

y	local coordinate normal to the surface
y^+	dimensionless wall distance
α	retention ratio
β_s	ozone removal rate by an individual surface
β_{total}	total ozone removal rate
γ	mass accommodation coefficient
Δy_1	distance of the first cell center from the surface
ε	turbulence dissipation rate
κ	Boltzmann constant (1.38×10^{-23} J/K)
λ, $\lambda_{outdoor}$, and $\lambda_{recirculated}$	total, outdoor, and recirculated air exchange rate
μ_t	turbulent viscosity
ρ	air density
$<v>$	Boltzmann velocity for ozone

1. Introduction

Aircraft passengers and crew could be exposed to a variety of chemical and biological agents during a flight. Many of the agents are potential health hazards (NRC, 2002). Ozone is one such chemical agent that poses a significant health concern (EPA, 2006; Weschler, 2006). Ozone exposure has been found to be associated with respiratory problems such as asthma, bronchoconstriction, airway hyperresponsiveness, and inflammation. (EPA, 2006). There is also suggestive evidence that links ozone to cardiovascular morbidity (EPA, 2006). Exposure to a low level of ambient ozone can increase mortality risk (Bell et al., 2006).

The risk of ozone exposure is high in an aircraft cabin environment because of the high ozone concentration in the air at typical cruise altitudes (500-800 ppb) and the subsequent ozone infiltration in the cabin through the air supply system. Ozone forms a variety of byproducts as a result of chemical reactions with human skin and with surfaces in aircraft cabins (Wisthaler et al., 2005; Weschler et al., 2007; Coleman et al., 2008; Pandrangi and Morrison, 2008; Wisthaler and Weschler, 2010). These chemical reactions can produce even more harmful chemical contaminants than the ozone itself (Weschler, 2004; Wisthaler et al., 2005) or secondary organic aerosols (Weschler and Shields, 1999).

To protect passengers and crew, the U.S. Federal Aviation Regulations (FAR Section 25.832) limit cabin ozone concentration to 250 ppb, sea level equivalent, at any time above flight level 320 (32,000 ft above sea level) or to 100 ppb, sea level equivalent, during any 3-h interval above flight level 270 (27,000 ft above sea level). To meet these regulations, some airlines employ catalytic converters in the air supply system to reduce the ozone level. However, in the absence or malfunctioning of these converters, the ozone level can go substantially higher. Spengler et al. (2004) measured the average ozone concentration in 106 flights and found that the ozone concentration in 20% of the flights exceeded the 100 ppb limit. Bhangar et al. (2008) collected real-time ozone data from 76 flights and found that ozone levels strongly varied with season and the presence or absence of an ozone converter.

In-flight measurements of ozone provide valuable information about the cabin air quality, but they are expensive and tedious. It is also difficult to identify the various factors affecting the ozone removal and byproduct formation through in-flight measurements. To overcome these difficulties, many investigations have used cabin mockups to systematically study ozone initiated reactive chemistry in a cabin environment (Wisthaler et al., 2005; Tamas et al., 2006; Weschler et al., 2007). These investigations have provided valuable information about the various factors that affect the cabin ozone levels and the ozone reactive chemistry. Although experimental studies provide reliable results, they are inflexible to changes in the system configuration and boundary conditions . It is also very difficult to obtain the distribution of ozone and associated byproducts in a cabin environment because of the large number of sensors required. Hence, it is necessary to develop a reliable and accurate method to calculate the ozone distributions and associated byproducts in a realistic cabin environment. The health risks to passengers and crew can then be assessed and possible mitigation strategies can be developed.

In order to understand the health risk to aircraft passengers from ozone, this research had a three-fold objective:

1. Develop a model to simulate the ozone distributions in an occupied aircraft cabin.
2. Compare the model results with available experimental data.
3. Use the model to study the ozone exposure of passengers.

2. Research Method

2.1. State of the Art

Many investigations have studied ozone distributions, the associated byproducts, and exposure assessments. For example, numerous experimental studies have been conducted to characterize ozone exposure and ozone initiated reactive chemistry in buildings and aircraft cabins (Wisthaler et al., 2005; Tamas et al., 2006; Wang and Morrison, 2006, 2010; Weschler et al., 2007; Wisthaler and Weschler, 2010). Wang and Morrison (2006, 2010) performed field experiments to quantify the emissions of ozone initiated aldehydes in buildings. They observed that ozone initiated emissions can continue for decades since indoor surfaces get replenished of reactive surface coating by various human activities. Weschler's group (Wisthaler et al., 2005; Tamas et al., 2006; Weschler et al., 2007) studied the ozone initiated reactive chemistry in an aircraft cabin mockup through a series of experiments. These experiments concluded that humans constitute an important site for ozone initiated reactive chemistry through the surface reaction of ozone with human skin oil. The experimental studies provided reliable results, but they were very expensive and cumbersome. Hence, some modeling studies have been attempted to provide a fast and convenient way to evaluate the indoor air quality.

Cano-Ruiz et al. (1993) developed an analytical model to determine the deposition of reactive gases at indoor surfaces. They obtained algebraic expression for deposition velocity under three airflow conditions and also performed a numerical simulation to further analyze the results. Weschler and Shields (2000) developed a mass balance model to study the influence of ventilation rate on the unimolecular and bimolecular chemical reactions occurring indoors, assuming perfectly mixed conditions. The results indicated that adequate ventilation is necessary, not only to remove pollutants generated indoors but also to limit chemical reactions in indoor air. The analytical models provide a quick and simple way to estimate the ozone contamination in an indoor environment. But it is difficult to solve analytically the model equations for complex indoor geometries and flow conditions without using the well mixed assumption.

Hence, several CFD modeling studies on ozone have been performed. Some researchers used CFD to analyze the volumetric and surface reactions of ozone in indoor settings (Sørensen and Weschler, 2002; Russo and Khalifa, 2010, 2011). They found significant spatial variations in the concentrations of reactants and products within the room and concluded that a well-mixed assumption might not be appropriate for many situations. A recent study by Rim et al. (2009) also used a CFD model to predict the ozone concentration in a breathing zone and ozone associated byproducts in a ventilated room. They found that ozone depleted in the breathing zone because of chemical reactions with human surfaces. These chemical reactions also led to an elevated level of byproducts in the breathing zone as compared to the bulk air.

The CFD studies provided a method to extend the analytical models to realistic indoor settings without using the well-mixed assumption. Nevertheless, the CFD studies were done for indoor environments that had a simple geometry with limited validations. Since numerical errors (discretization error, computer round-off error, etc.) and modeling errors (turbulence model errors, unknown boundary conditions, etc.) could affect the accuracy of the CFD results, solid validation of the CFD results with reliable experimental data is clearly necessary. The above review shows that, in order to study ozone reaction and its byproducts formed in an aircraft cabin, CFD seems to be a good method, but experimental data are needed to validate the results.

2.2. CFD Governing Equations

This investigation used CFD to model the ozone transport and deposition since it is inexpensive and informative. CFD solves the Reynolds-averaged Navier-Stokes equations with the Re-Normalization Group (RNG) k-ε turbulence model (Yakhot and Orszag, 1986). Zhang et al. (2009) recommended using the RNG k-ε turbulence model since it can effectively predict the turbulent features of the airflow in an aircraft cabin. The ozone concentration distribution was solved by the following species transport equation:

$$\nabla.(\rho\vec{u}C) = \nabla.((\rho D_o + \frac{\mu_t}{Sc_t})\nabla C) + S_c \quad (1)$$

where ρ is air density, $\vec{u}$ air velocity vector, C ozone concentration, D_o binary diffusion coefficient of ozone in air, μ_t turbulent viscosity, Sc_t turbulent Schmidt number, and S_c ozone source.

This investigation used the second-order upwind discretization scheme for solving all the variables except pressure. Pressure discretization was based on the PRESTO! (PREssure STaggering Option) scheme (FLUENT, 2009). The governing equation equations were solved using the SIMPLE algorithm (Patankar, 1980) in the commercial CFD software FLUENT (FLUENT, 2009).

2.3. Surface Deposition

In order to solve the ozone distribution in an aircraft cabin by using Eq. (1), it is necessary to have an appropriate model to compute the ozone deposition (or removal) at cabin and human related surfaces. The surface ozone deposition depends on (1) fluid motion and ozone diffusion that transport ozone molecules to the surfaces and (2) the ozone chemical reactions on the surfaces. The ozone deposition flux at surface J_s is given by (Cano-Ruiz et al., 1993):

$$J_s = -\gamma.\frac{<v>}{4}.C\Big|_{y=\frac{2}{3}l} \quad (2)$$

where γ is the mass accommodation coefficient (or reaction probability) between the ozone and the deposition surface and is defined as the fraction of all ozone molecules collision with the surface that results in deposition, $<v>$ Boltzmann velocity for ozone ($<v> = \left(\frac{8.\kappa.T}{\pi.m}\right)^{1/2}$), C ozone concentration, and l mean molecular free path (6.5×10^{-8} m at 293 K and 1 atm).

Eq. (2) can be used to calculate the ozone flux at cabin and human related surfaces. However, Eq. (2) requires CFD to use an extremely fine grid size near the deposition surface (comparable to l). To increase the grid size near the surface, this study used the following flux model (Sørensen and Weschler, 2002):

$$J_s = \frac{-\gamma.\frac{<v>}{4}}{1+\gamma.\frac{<v>}{4}.\frac{\Delta y_1}{D_o}}.C\Big|_{y=\Delta y_1} \quad (3)$$

where Δy_1 is the distance of the first cell center from the surface. Note that Eq. (3) is valid only when the first grid point is very close to the surface (ideally $y^+<1$).

This study used Eq. (3) to determine the ozone flux at cabin surfaces such as the carpet and seats. Since ozone reacts significantly with human related surfaces such as skin, hair, and clothing (Wisthaler et al., 2005; Weschler et al., 2007; Pandrangi and Morrison, 2008), the ozone concentration is expected to be very low at those human related surfaces (Pandrangi and Morrison, 2008). Hence, this study set zero ozone concentration at human related surfaces, as suggested by Rim et al. (2009).

2.4. Mass accommodation coefficient (*γ*)

The γ for different surfaces is a necessary input for the CFD model to compute the ozone deposition using Eq. (3). The γ was calculated by using the two-resistor model developed by Cano-Ruiz et al. (1993):

$$\gamma = \left[\frac{<v>}{4}.\left(\frac{1}{v_d} - \frac{1}{v_t}\right)\right]^{-1} \quad (4)$$

where v_d is the ozone deposition velocity and defined as the ozone flux normalized by a characteristic ozone concentration; v_t the transport limited deposition velocity and defined as the deposition velocity when γ equals one.

The v_d for the different surfaces was available from the experimental data of Tamas et al. (2006). The v_t was estimated using CFD as follows:

1. The v_d is equal to v_t, when the surface resistance to the ozone deposition becomes zero; i.e., the surface becomes a perfect sink.
2. Hence, in order to estimate v_t for a surface, we performed CFD simulations by setting the ozone concentration equal to zero at that surface.
3. The v_d (which equals to v_t) was calculated by the following equation:

$$v_d = \frac{Q}{A}\frac{(C_{inlet} - C_{outlet})}{C_{cabin}} \quad (5)$$

where Q is the supply airflow rate to the cabin; A the area of the ozone deposition surface; and C_{inlet}, C_{outlet}, and C_{cabin} the inlet, outlet, and volume averaged cabin ozone concentrations, respectively. Note that the above equation is valid for a cabin with only one deposition surface, one inlet, and one outlet, under steady state.

The γ for the carpet surface is 8.4×10^{-6} by using the above-mentioned method. The value is lower than that of some previous measurements made for carpet surfaces (Morrison and Nazaroff, 2000; Coleman et al., 2008), where γ was found to be between 10^{-4} and 10^{-5}. The study by Morrison and Nazaroff (2000) also found that all carpet specimens exhibited the phenomenon of "aging" since the γ decreased after a long period of ozone exposure. The γ obtained in this investigation is comparable to that of carpet surfaces obtained after 48-hour ozone exposure (Morrison and Nazaroff, 2000). A direct comparison between these different γ values should be avoided as different studies used different carpet specimens that had a wide variety of storage and usage history.

The γ for seat surfaces was determined to be 1.9×10^{-5}, which is lower than that obtained experimentally by Coleman et al. (2008) for a soiled seat fabric ($\gamma = 1.4\times10^{-4}$). Again, the differences could be attributed to the differences in seat fabric and usage history. Nevertheless, the γ for seat surfaces is higher than that for carpet since the seat fabric is soiled with human skin oils to some extent. These γ values for carpet and seat surfaces have been used in this study to compute the ozone deposition by using Eq. (3).

3. Case Setup

This investigation used CFD to simulate the ozone distributions in an aircraft cabin mockup for which detailed experimental data were available (Tamas et al., 2006). The cabin mockup was a section of Boeing-767 (3 rows, 21 seats) as shown in Fig. 1, which was 4.9 m wide, 3.2 m long, and 2.0 m high in the center with a total volume of $28.5 m^3$. The experimental setup injected the air containing ozone to the cabin from the two overhead air-supply slots along the longitudinal direction (12 mm × 3200 mm each) with a velocity of 2.6 m/s and a flow rate of 200 L/s. The ozone concentration in the cabin mockup was measured at its center and varied from 41-341 ppb depending on the experimental conditions and objectives, but this investigation used only a constant ozone concentration of 100 ppb at the inlets. Note that the species transport equation (Eq. (1)) and the CFD boundary conditions used in this investigation were homogeneous (if 'C' is a solution, then all its multiples will also be solutions) with respect to the ozone concentration except the inlet condition. Hence, the absolute level of ozone would be determined by the inlet concentration and all the results can be normalized with the volume averaged cabin ozone concentration for comparison against the experimental data.

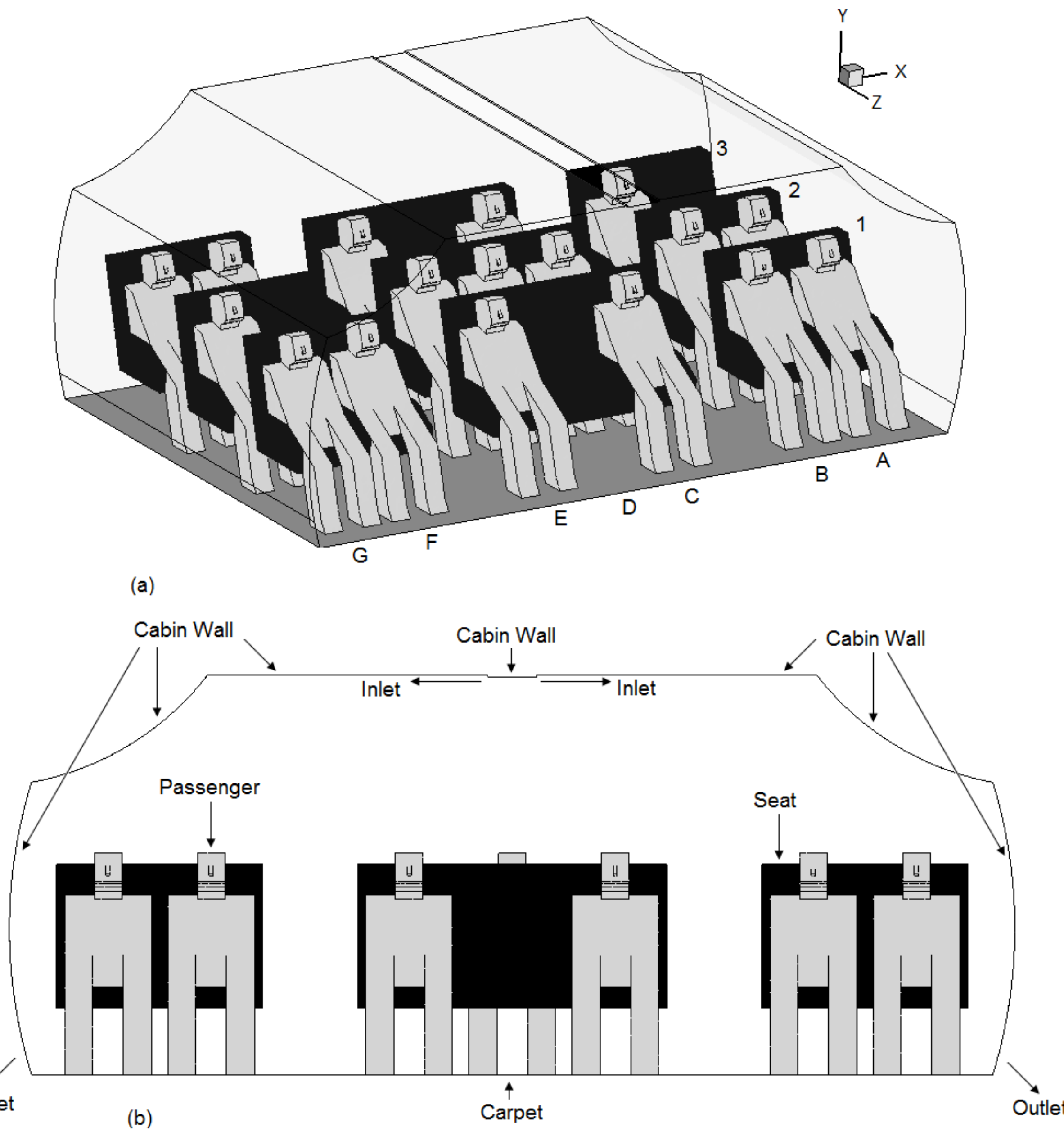

Fig. 1: The occupied cabin setup for Case 5, (a) the schematic of the case and (b) boundary surfaces in the cabin mockup.

In the experiment, the air containing ozone entered the cabin mockup through the air supply system. The ozone in the cabin depleted due to its reaction with various surfaces (carpet, seats, human skin, and clothing) and gas phase compounds. The ozone removal by surface reaction versus gas phase reactions was governed by the outdoor air exchange rate. The high outdoor air exchange rate (between 3.0 and 8.8 ACH) in the cabin reduced the time available for gas phase reactions because the residence time of the gases in the cabin was low. At such high outdoor air exchange rates, only unsaturated organic compounds can undergo gas phase reactions with ozone. Weschler et al. (2007) measured the level of unsaturated organic compounds in the cabin mockup at outdoor air exchange rates of 4.4 and 8.8 ACH in the absence of ozone (ozone concentration less than 2 ppb). They found that the concentration of unsaturated organic compounds was very low (less than 2 ppb) for any significant loss of ozone through gas phase reactions. Thus, the high air exchange rate in the cabin coupled with the low concentration of unsaturated organic compounds prevented the ozone removal by gas phase reactions. Hence, the present investigation only modeled the ozone removal by surface reactions.

In order to separate the influence of each surface on the ozone concentration, this investigation designed five different cases as illustrated in Table 1.The cabin setup in the design varied systematically, such as the presence or absence of seats and people and soiled T-shirts. The gradual changes in the complexity of the boundary conditions in these cases enabled us to make a step-by-step comparison with the experimental data for validating the CFD model. The occupied cabin cases (Cases 4 and 5) were designed to gain an understanding of the exposure to ozone of passengers seated at different locations in the cabin as well as the overall ozone distribution in the cabin environment. The boundary conditions in the CFD model are presented in Table 2. The enhanced wall treatment model (FLUENT, 2009) was used to solve the airflow near the walls. The inlet temperature was 24°C for Cases 1, 2, and 3 and 21.2°C for Cases 4 and 5. The lower temperature in Cases 4 and 5 was to maintain the same cabin air temperature by offsetting the heat generated by the passengers. Figure 1 shows the schematic and its boundary surfaces for Case 5, which represented the most complex scenario. Figure 2 shows the grid used for Case 5. The grid consisted of 2.43 million elements where tetrahedral elements were used for the bulk volume, and layers of extruded triangular prisms were created on ozone reactive surfaces. The prism elements were used near the ozone reactive surfaces to accurately capture the boundary layer flow and ozone deposition. The initial height of the prism layer was kept very small (~2 mm) to ensure that the y^+ was small (~5) near the ozone reactive surfaces, and the deposition model (Eq. (3)) was valid. The average y^+ for the other cabin surfaces was around 15 and the maximum value was less than 100 in all the cases. This meshing strategy was used for all the cases.

Table 1: Description of the five cases used in studying the ozone reaction in a cabin mockup

Case	*Description*	*Ozone reaction surfaces*
1	Empty cabin	Carpet
2	Cabin with seats	Carpet and seats
3	Cabin with seats and T-shirts	Carpet, seats, and T-shirts
4	Occupied cabin with simple human geometry (block model)	Carpet, seats, and passengers
5	Occupied cabin with detailed human geometry	Carpet, seats, and passengers

Table 2: The thermal, ozone, and turbulence boundary conditions used for the five cases

Surfaces	*Temperature*	*Ozone*	*Turbulence*
Inlet	Case specific	100 ppb	$k = 3/2(0.1U_{in}^2)$, $\varepsilon = (C_\mu k_{in}^{3/2})/L_{in}$ $C_\mu = 0.09$, L_{in}=*(Air supply slot width)/7*
Cabin walls	18°C	Zero flux	$\partial k/\partial y = 0$, *ε: local equilibrium hypothesis*
Outlets	Outflow	Outflow	Outflow
Carpet	18°C	Flux calculated with Eq. (3)	$\partial k/\partial y = 0$, *ε: local equilibrium hypothesis*
Seats	Adiabatic	Flux calculated with Eq. (3)	$\partial k/\partial y = 0$, *ε: local equilibrium hypothesis*
T-shirts	Adiabatic	Zero concentration	$\partial k/\partial y = 0$, *ε: local equilibrium hypothesis*
Passengers	31°C	Zero concentration	$\partial k/\partial y = 0$, *ε: local equilibrium hypothesis*

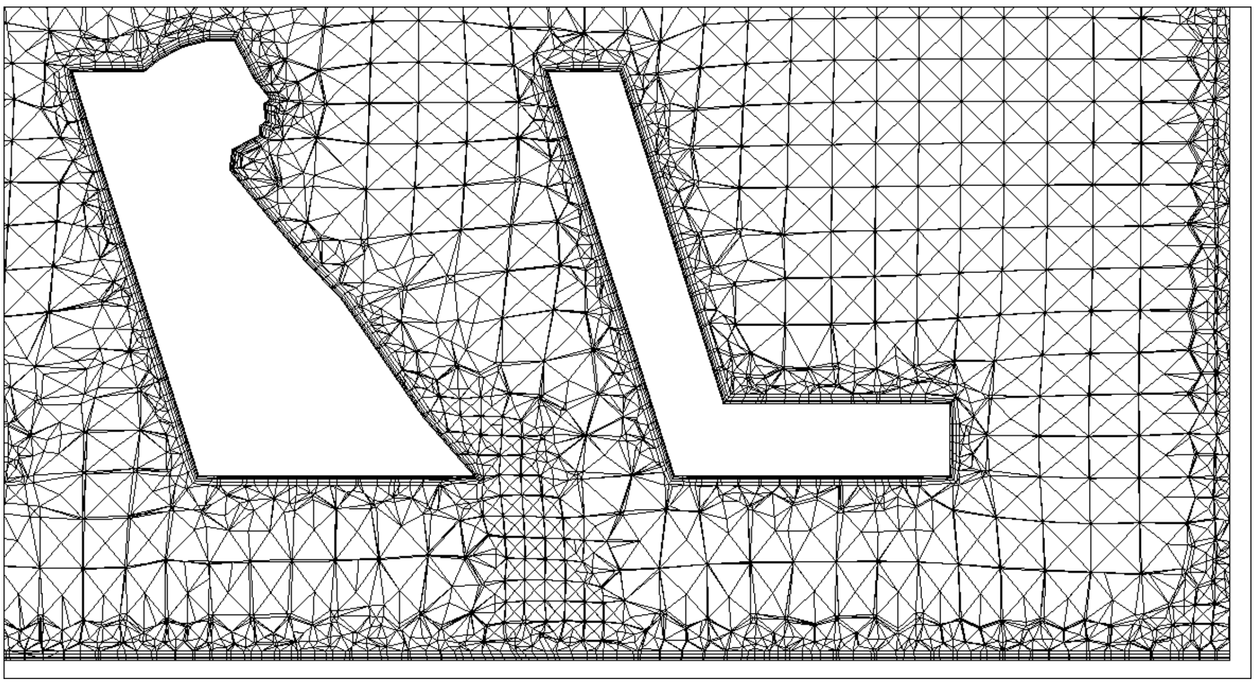

Fig. 2: Mesh distribution in the longitudinal section through the cabin center for Case 5.

Our study simulated the passengers by two different human geometry models for the occupied cabin cases. Case 4 used a simple block model, while Case 5 used a more detailed representation of human shape, as shown in Fig. 3. The two geometric models were designed to identify whether the simple block model was sufficient for CFD modeling. Fig. 3 also depicts a breathing zone of 500 cm^3 volume below the nose since this investigation assessed the ozone dose inhaled by the passengers by calculating the volume-averaged concentration in the breathing zone as suggested by Rim et al. (2009). The volume of breathing zone was chosen larger than the hemispherical volume suggested by Brohus (1997) to account for the face movements of passengers.

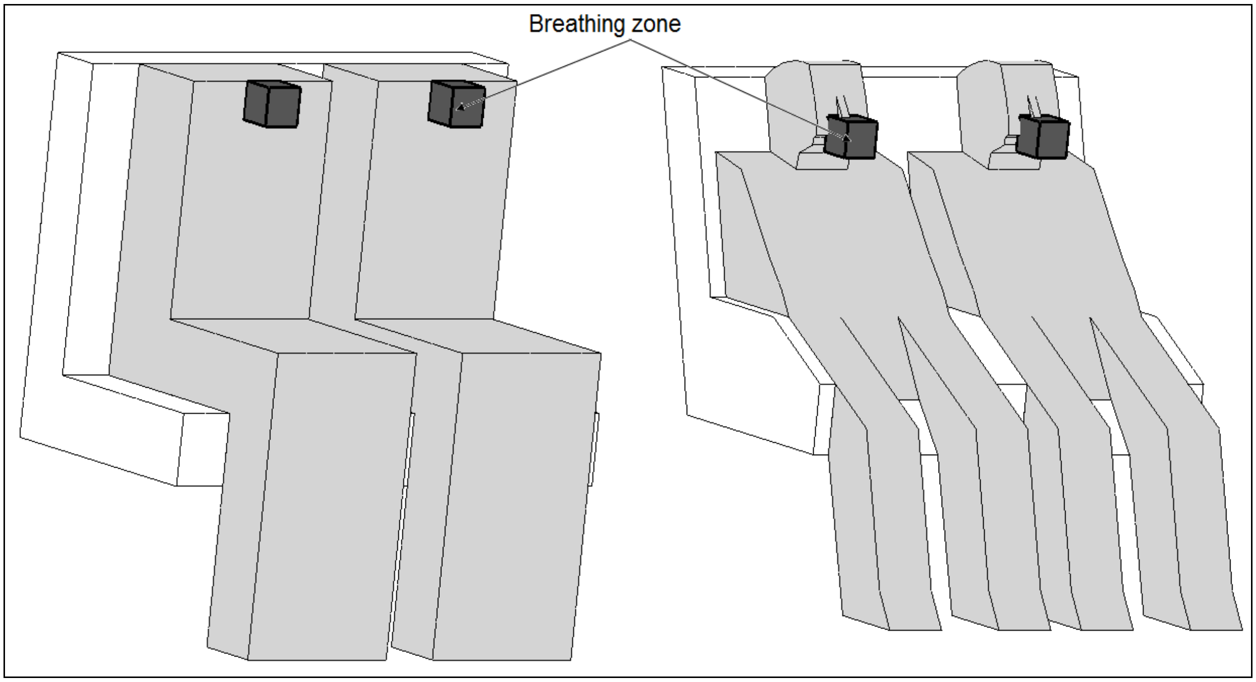

Fig. 3: Occupant geometries and breathing zones for Cases 4 and 5

4. Evaluation Parameters

This section defines some important parameters for evaluating the cabin air quality for the cases designed in the previous section. These parameters help evaluate the CFD results against the available experimental data.

4.1. Total ozone removal rate (**β_{total}**)

The total ozone removal rate (β_{total}) quantifies the total ozone loss in the cabin environment due to surface and gas phase reactions. Under steady state conditions β_{total} is given by:

$$\beta_{total} = \lambda \frac{(C_{inlet} - C_{outlet})}{C_{cabin}} \quad (6)$$

where λ is the total air exchange rate (the sum of the outdoor and recirculated air exchange rate). According to this definition, the β_{total} can be obtained experimentally by measuring the ozone concentrations or computationally by calculating the ozone concentrations from CFD.

The β_{total} can also be obtained by measuring the first order decay of ozone inside the cabin. In this method, ozone is injected into the cabin until a reasonable ozone concentration (roughly around 50-100 ppb) is reached. The ozone injection is then stopped and the cabin ozone concentration is measured with respect to time. The ozone decay in the cabin is quantified by a best fit to an exponential decay equation given by:

$$C_t = C_{t=0} . e^{-(\lambda_{outdoor} + \beta_{total}).t} \quad (7)$$

where C_t is the ozone concentration at time t; $C_{t=0}$ is the concentration at the time when the ozone injection was stopped; $\lambda_{outdoor}$ is the outdoor air exchange rate. The decay constant ($\lambda_{outdoor} + \beta_{total}$) in the above equation can be used to determine β_{total} when the $\lambda_{outdoor}$ is known. The experimental study by Tamas et al. (2006) obtained the β_{total} primarily by using Eq. (7), and Eq. (6) was used when steady state conditions were achieved.

4.2. Contribution to ozone removal rate (β_s)

The contribution to the ozone removal rate (β_s) quantifies the ozone removal by an individual surface. It is defined as:

$$\beta_s = \frac{\int J_s dA}{C_{cabin} . V_{cabin}} \quad (8)$$

where V_{cabin} is the volume of the air inside the cabin. The β_s definition implies that it can be calculated from CFD but cannot be directly measured, since the surface ozone deposition (the numerator in Eq. (8)) is difficult to quantify. Therefore, to determine β_s, a reacting surface should be added one at a time. This is why the investigation designed five cases. In case 1, the β_s can be approximated as follows if the gas phase reactions of ozone are neglected:

$$\beta_{s\,carpet} = \beta_{total\,Case1} \quad (9)$$

By adding the reacting surfaces one at a time in Cases 2, 3, and 4, the β_s for seats, T-shirt, and passengers can be estimated as:

$$\beta_{s\,seats} = \beta_{total\,Case2} - \beta_{s\,carpet} \quad (10)$$

$$\beta_{s\,T-shirts} = \beta_{total\,Case3} - \beta_{s\,carpet} - \beta_{s\,seats} \quad (11)$$

$$\beta_{s\,passengers} = \beta_{total\,Case4} - \beta_{s\,carpet} - \beta_{s\,seats} \quad (12)$$

Hence, the experimental β_s values can be compared with those obtained from CFD (Eq. (8)). Note that Eqs. 10, 11 and 12 used in the experimental study (Tamas et al., 2006) implicitly assume that the ozone deposition on one surface does not affect deposition on other surfaces.

4.3. Ozone deposition velocity (v_d)

The deposition velocity (v_d) characterizes the intensity of ozone surface reactions and can be compared to those reported in the literature. It is analogous to the heat transfer coefficient as:

$$v_d = \frac{J_s}{C_{cabin}} \quad (13)$$

where J_s and C_{cabin} are analogous to the heat flux and temperature difference. According to Eq. (13), v_d will vary across a surface as the ozone flux (J_s) will vary depending on the position. Hence, it is convenient to define v_d by using the average ozone flux over a surface (or multiple surfaces) as:

$$v_d = \frac{(\int J_s dA) / A}{C_{cabin}} \quad (14)$$

Similar to β_s, the v_d can also be calculated from CFD, but cannot be measured directly. Hence, by combining Eqs. (8) and (14), v_d can be determined as:

$$v_d = \frac{\beta_s . V_{cabin}}{A} \tag{15}$$

4.4. Retention ratio (*α*)

The retention ratio (α) is a parameter that indicates the ozone loss in the aircraft due to reactions in the cabin and the air supply system in the absence of ozone converters. It is defined as:

$$\alpha = \frac{C_{cabin}}{C_{ambient}} \tag{16}$$

where $C_{ambient}$ is the ambient ozone concentration. If the ozone reactions in the air supply system are neglected, then $\lambda . C_{inlet} = \lambda_{outdoor} . C_{ambient} + \lambda_{recirculated} . C_{outlet}$. Eq. (16) can be rearranged to give:

$$\alpha = \frac{\lambda_{outdoor} . C_{cabin}}{\lambda . C_{inlet} - \lambda_{recirculated} . C_{outlet}} \tag{17}$$

where $\lambda_{outdoor}$ is the outdoor air exchange rate; $\lambda_{recirculated}$ the recirculated air exchange rate. The experiment used Eq. (16) to determine α from the measured C_{cabin} and $C_{ambient}$. But this investigation used Eq. (17) to calculate α, since the air supply system was not modeled.

4.5. Ozone ratio (r_{ozone})

In order to quantify the ozone dose for different passengers, it is essential to calculate the ozone concentration in the breathing zone. This study used ozone ratio (r_{ozone}) to compare the inhaled ozone concentration with the average ozone concentration in the cabin:

$$r_{ozone} = \frac{C_{BZ}}{C_{cabin}} \tag{18}$$

where C_{BZ} is the ozone concentration in the breathing zone. The r_{ozone} can be used for assessing the health risk in the cabin based on the average ozone concentration.

5. Results

The following section reports how the CFD was used to obtain the evaluation parameters defined in Section 4 and shows the comparison with the experimental data from Tamas et al. (2006).

5.1. Ozone removal by carpet and seats (Cases 1 and 2)

Cases 1 and 2 were designed for identifying the ozone removal by the cabin surfaces (carpet and seats) by adding them one by one.

In Case 1, the carpet was assumed to be the only ozone reactive surface to determine its β_s and v_d. Hence, the measured β_{total} and the β_s calculated by Eq. (8) should be equal. This investigation calculated that the β_s for the carpet was 1.07 h^{-1}. The β_s calculated and the β_{total} measured were indeed nearly the same as shown in Fig. 4. The v_d for the carpet was calculated by using Eq. (14) as 0.06 cm/s, which also agreed with the measurements as shown in Fig. 5.

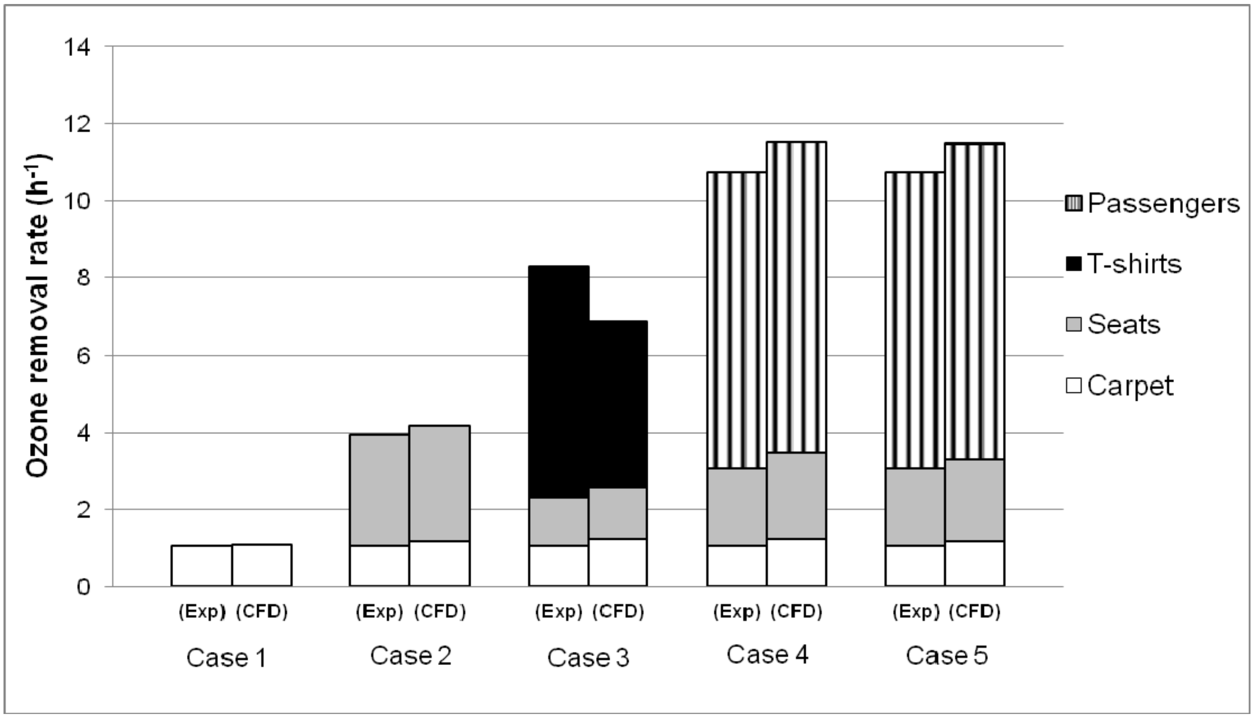

Fig. 4: Comparison of the computed ozone removal rate with the corresponding experimental data from Tamas et al. (2006) for various cabin and human related surfaces.

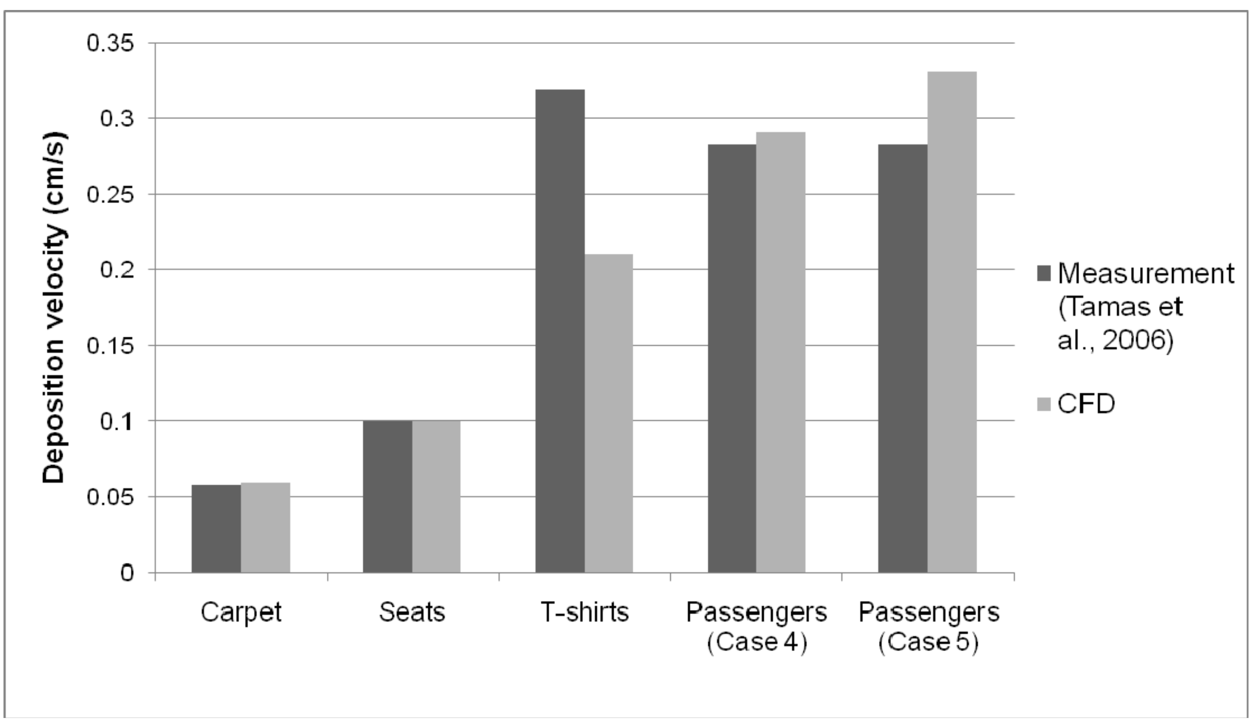

Fig. 5: Comparison of the computed deposition velocity with the corresponding experimental data from Tamas et al. (2006) for various cabin and human related surfaces.

In Case 2, the seats were also placed in the cabin together with the carpet. This was done in the experiment to determine the β_s for the seats by using Eq. (10) since the β_s for the carpet was assumed to be known from the previous case. This investigation calculated the β_s for the carpet and seats as 1.19 h^{-1} and 2.97 h^{-1}, respectively, by using Eq. (8). The seats had a higher β_s than the carpet because they had a larger surface area for reaction and also a higher reactivity. The β_{total} was greater than Case 1 because of the additional ozone removal by the seats. The computed β_s and β_{total} agreed with the measured data as shown in Fig. 4. The v_d for the carpet and seats was calculated by using Eq. (14) as 0.06 cm/s, and 0.10 cm/s, respectively, which also agreed with the measurements as shown in Fig. 5. Hence, the "measured" β_s and v_d for the seats seem correct, and the CFD results are also reliable.

The β_{total} and v_d for Case 2 (which represents a typical unoccupied cabin setup) can also be compared to those in buildings to better understand the ozone depletion in the cabin and the reactivity of the cabin surfaces. Lee et al. (1999) measured the average β_{total} as 2.80 ± 1.30 h^{-1}, and v_d as 0.049 ± 0.017 cm/s in the living rooms of 43 Southern California homes. The v_d measured by Lee et al. (1999) included all indoor surfaces (including both ozone reactive and inert surfaces). If the same method is applied to this cabin, the v_d for both ozone reactive and inert surfaces is 0.04 cm/s. Note that although the v_d for the cabin was almost the same as that for the homes, the β_{total} for the cabin was 1.5 times higher than that for the homes. This is because the V/A in Eq. (15) for the cabin was lower than that for the homes.

5.2. Ozone removal by T-shirts soiled with human skin oil (Case 3)

This case was designed for identifying the ozone removal by clothing soiled with human skin oil. The cabin in Case 3 was identical to the one in Case 2, except that the seat backs were covered with T-shirts. The T-shirts were soiled with human skin oil as male subjects had slept in them overnight.

The β_s for the carpet, seats, and T-shirts were 1.23 h^{-1}, 1.34 h^{-1}, and 4.29 h^{-1}, respectively, calculated by Eq. (8). The area of the T-shirts was approximately 40% of all the surface areas, but it removed about 60% ozone due to the high reactivity of ozone with squalene in human skin oil. The β_{total} was higher than that in previous cases because of the addition of the T-shirts. The experiment used Eq. (11) to determine $\beta_{s\ T\text{-}shirts}$, with β_{s_carpet} and β_{s_seats} from Cases 1 and 2. However, it is not appropriate to use the β_{s_seats} obtained in Case 2 to calculate $\beta_{s\ T\text{-}shirts}$, since a large area of the seats was covered with the T-shirts and was not part of the ozone reaction in Case 3. Thus, this investigation used the following procedure to determine the "measured" $\beta_{s\ T\text{-}shirts}$:

1. The $\beta_{s\ seats}$ for Case 3 was assumed to be proportional to the exposed area, which was available for ozone reactions.
2. Since the exposed area of the seats was unknown, it was assumed to be equal to that used in the CFD investigation, which was about 45% of the total area.
3. The "measured" $\beta_{s\ seats}$ was determined by using $\beta_{s\ seats,\ Case\ 3} = \beta_{s\ seats,\ Case\ 2} \times (A_{exposed}/A_{total})$, where $A_{exposed}/A_{total}$ is the ratio of the exposed area to the total area of the seats.
4. The "measured" $\beta_{s\ T\text{-}shirts}$ was then determined from the $\beta_{s\ seats}$ obtained in the previous step by using Eq. (11).

The comparison between the "measured" β_s obtained using the above procedure and the CFD results is shown in Fig. 4. The computed $\beta_{s\ carpet}$ and $\beta_{s\ seats}$ agreed well with the measurements but the computed $\beta_{s\ T\text{-}shirts}$ and β_{total} were underestimated by CFD. A possible reason for these discrepancies could be that when ozone reacted with the human skin oil present in T-shirts, some of the volatile byproducts that entered the gas phase reacted further with the ozone (Weschler et al., 2007). This gas phase chemistry could have contributed to the additional ozone removal in the experiment, but was not considered in the CFD analysis.

The computed v_d for the T-shirts was 0.21 cm/s by using Eq. (14), and the computed v_d for the carpet and seats remained the same as in the previous cases (0.06 cm/s and 0.1 cm/s, respectively). The high value of v_d for the T-shirts shows that the ozone reaction intensity was very high at the surfaces. In order to compare the CFD results with the measurements, this investigation used the "corrected" $\beta_{s\ T\text{-}shirts}$ to calculate the "measured" $v_{d\ T\text{-}shirts}$ by using Eq. (15). Since the CFD underpredicted the $\beta_{s\ T\text{-}shirts}$, the $v_{d\ T\text{-}shirts}$ was also lower than the measured one, as shown in Fig. 5.

5.3. Ozone removal by passengers (Cases 4 and 5)

Cases 4 and 5 were designed for identifying the ozone removal in an occupied cabin mockup. The only difference between them was: Case 4 represented passengers by simple block models, whereas Case 5 had a more detailed representation of human geometry, as shown in Fig. 3. Despite the differences in the human geometric presentation, the area available for ozone reaction remained approximately the same.

The β_s for the carpet, seats, and passengers calculated from Eq. (8) was 1.23 h^{-1}, 2.25 h^{-1}, and 8.03 h^{-1}, respectively, in Case 4; and it was 1.18 h^{-1}, 2.12 h^{-1}, and 8.18 h^{-1}, respectively, in Case 5. The small differences in β_s between Cases 4 and 5 show that the detailed representation of occupant geometry for the CFD studies was not important for evaluating the ozone removal rate as long as the reactive surface area was the same. The β_{total} for the two cases was significantly greater than those in all the previous cases due to the large contribution of the passengers to ozone removal.

In order to compare the β_s with the experimental data, this investigation used the procedure described in Case 3 to correct the measured $\beta_{s\ seats}$ and determine the "measured" $\beta_{s\ passengers}$ by using Eq. (12). Fig. 4 compares β_s and β_{total} obtained by CFD and the measurements. The computed $\beta_{s\ carpet}$ and $\beta_{s\ seats}$ agreed well with the measurements, but the CFD overpredicted the $\beta_{s\ passengers}$ and β_{total} by 10%.

The v_d for the passengers was computed by using Eq. (14) to be 0.29 cm/s and 0.33cm/s for Cases 4 and 5, respectively. The computed v_d for the carpet and seats was the same as those in the previous cases (0.06 cm/s and 0.1 cm/s, respectively). Similar to $v_{d\ T\text{-}shirts}$, the high v_d for the passengers showed that the ozone removal by the passengers was most important or the reactivity of the passengers was the highest. The "measured" $v_{d\ passengers}$ was determined from the corrected $\beta_{s\ passengers}$, based on the exposed surface area of the passengers (estimated at about 1.2 m^2 per passenger) and the volume of the cabin air (estimated at about 27 m^3) by using Eq. (15). Since the CFD results overpredicted the $\beta_{s\ passengers}$, Fig. 5 shows that the $v_{d\ passengers}$ was also overpredicted.

This investigation computed α as 0.42 for an outdoor airflow rate (8.8 h^{-1}) in Case 5 by using Eq. (17). The α for Case 4 was approximately equal to Case 5. The calculated α was less than that reported in the experiment (0.21) because the ozone removal in the air supply system was not modeled. The α was smaller than the default value of 0.7 used by the Federal Aviation Administration (FAA) for determining the cabin ozone concentration and showing compliance with regulations. The low α indicated that the cabin ozone concentration should be lower than that specified by the FAA. But this reduction in the cabin ozone levels was accompanied by the formation of even more harmful volatile byproducts (Weschler, 2004; Wisthaler et al., 2005). Hence, a low α may reduce health risks from ozone inhalation, but would increase them from its byproducts.

Fig. 6 shows the ozone distribution along the longitudinal plane through the center of the cabin in Case 5. It shows that ozone depleted near the carpet, seats, and breathing zone of the passenger because of the surface chemical reactions. This investigation used r_{ozone} to quantify the breathing zone ozone concentration for the passengers as compared to in the average cabin concentration. The r_{ozone} varied between 0.77 - 0.93 in Case 4 and 0.77 - 0.99 in Case 5. The averaged r_{ozone} for all the passengers was 0.85 and 0.90 for Cases 4 and 5, respectively, which is in qualitative agreement with previous studies. (Liu et al., 1994; Rim et al., 2009).The breathing zone concentration is generally lower than the average ozone concentration in the indoor environment (r_{ozone} <1) because of reactions at the human surfaces. The r_{ozone} varied among the aircraft passengers due to the differences in the ozone transport and surface reactions at different locations. Fig. 7 compares the r_{ozone} for different passengers between the two cases, which shows r_{ozone} being quite sensitive to human geometrical representations. Since most of the passengers inhaled an ozone concentration lower than the average one, it is better to use the local ozone concentration if one wants to accurately assess the health risks associated with the ozone.

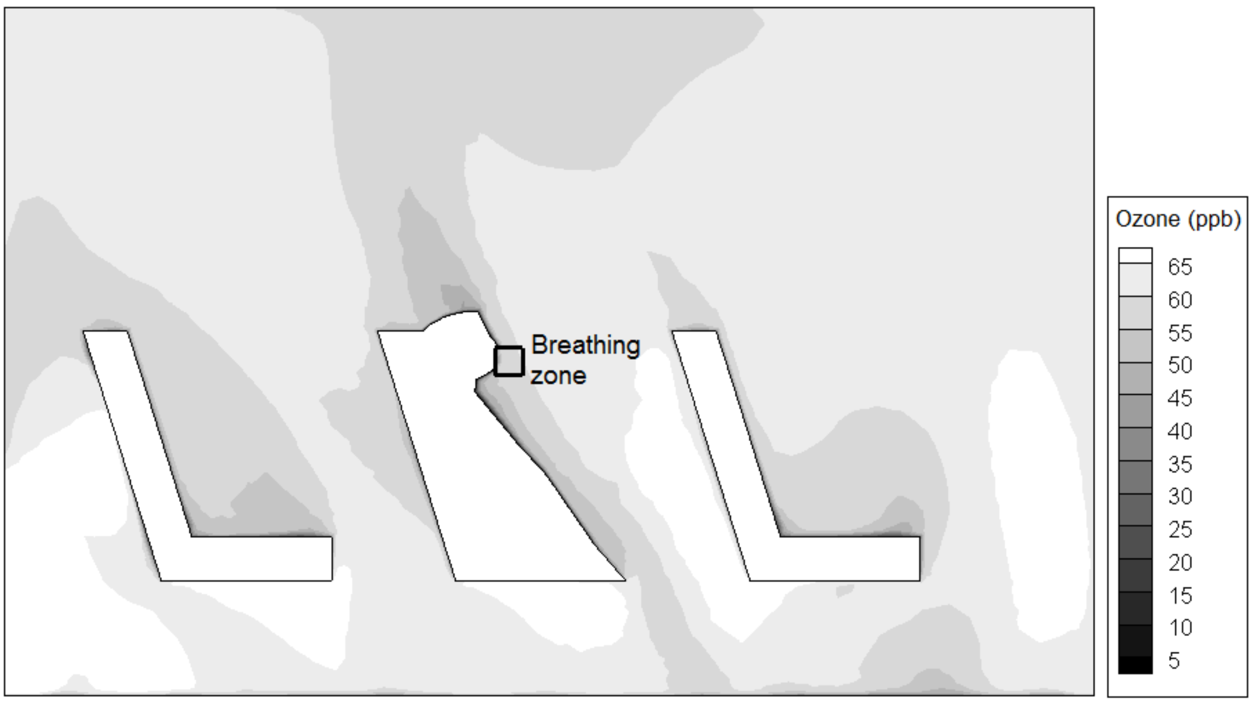

Fig. 6: Ozone distribution in the longitudinal section through the cabin center

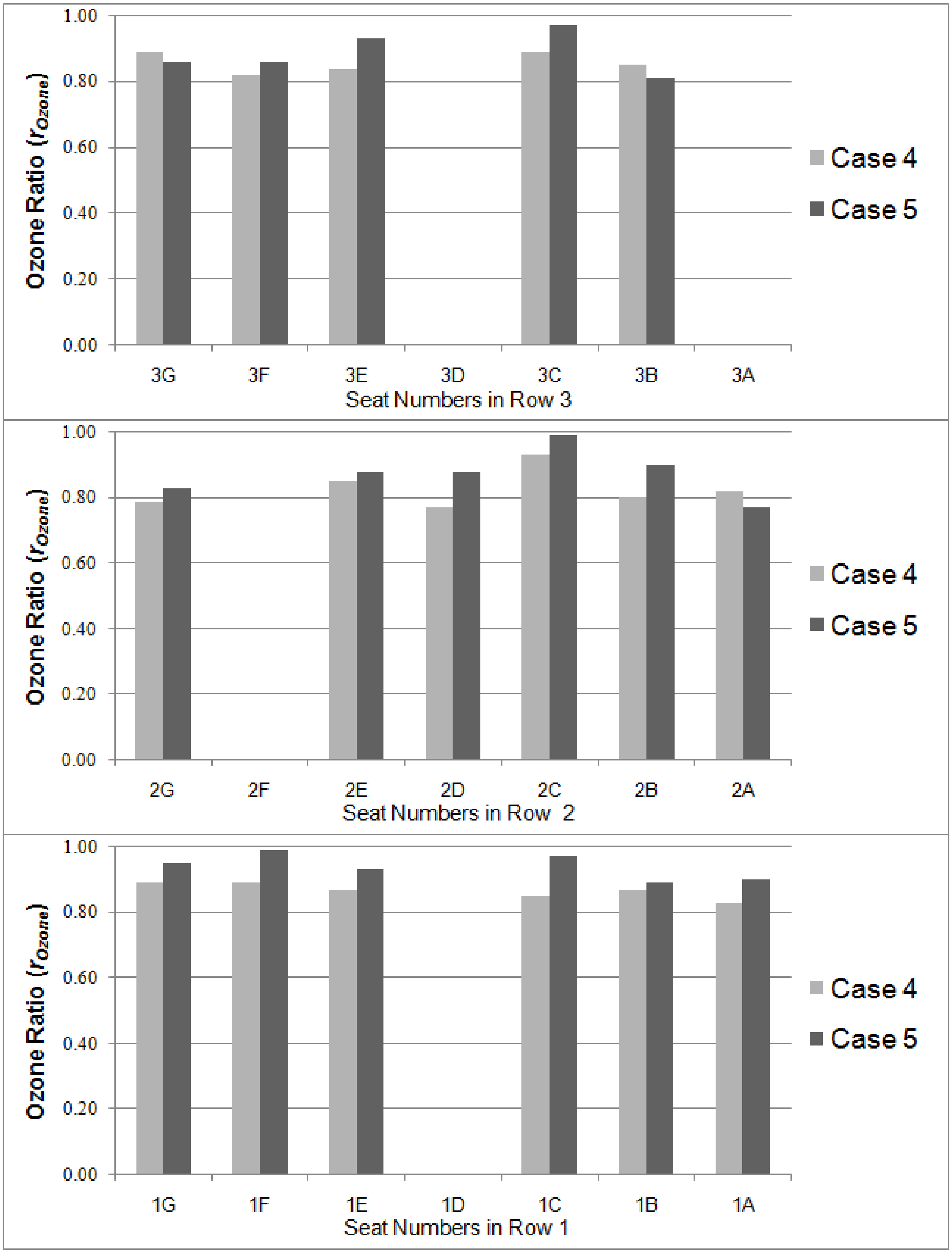

Fig. 7: Comparison of ozone ratio (r_{ozone}) for the passengers in the breathing zone between Cases 4 and 5. Seats 1D, 2F, 3A, and 3D were unoccupied.

6. Discussion

The primary difficulty in computing the ozone distribution was that the γ for the ozone reactive surfaces was unknown. Hence, this investigation obtained the γ from the "measured" v_d and computed v_t by using Eq. (4). The flux model (Eq. (3)) was then used to compute the ozone removal by cabin surfaces. However, in the cases with the T-shirts and passengers, the flux model (Eq. (3)) was not used to compute the surface deposition since the v_d was found to be very close to v_t, and Eq. (4) was not suitable. Instead, a zero ozone concentration was assumed on the human related surface. Since the computed β_s and v_d agreed with the measured data, our method seems acceptable.

This study also performed grid independence analysis for the CFD simulations. For example, in Cases 2 and 3 where the cabin geometry was identical, this investigation used a coarse grid of 2.31 million elements and a fine grid of 4.96 million elements for the two cases. The initial prism layer height was 2 mm and 1 mm, for the coarse and fine grid, respectively. The velocity and ozone distributions obtained with the two grid sizes were similar and the difference between the computed ozone removal rates (β_{total}) was less than 5%. Thus, the coarse grid was selected for performing all CFD simulations reported in this paper.

7. Conclusions

The investigation developed a CFD model to study the ozone reactions at different cabin and human related surfaces and simulate the ozone distributions in the cabin. The investigation led to the following conclusions:

- The study identified the individual contributions of cabin and human related surfaces to ozone removal and their deposition velocities. The results concluded that the human related surfaces (T-shirts and passengers) removed much more ozone than the cabin surfaces (carpet and seats).
- The ozone removal rate and deposition velocities calculated by the model were in good agreement with those measured by Tamas et al. (2006).
- The retention ratio predicted by the model was higher than the measured one (Tamas et al., 2006) since the air supply system was not modeled. The retention ratios were lower than the FAA recommended value, indicating a reduced risk directly from ozone inhalation but an increased risk from associated by-products.
- Ozone depleted more in the breathing zone compared to the average cabin concentration due to reaction at the human surfaces. To accurately assess the personal exposure to ozone, its concentration in the breathing zone should be used.

Acknowledgements

The authors would like to thank Dr. Charles J. Weschler of the University of Medicine and Dentistry of New Jersey for his help in interpreting the experimental data obtained by his group and our CFD results. This study was partially supported by the National Basic Research Program of China (The 973 Program) through grant No. 2012CB720100 and partially funded by the U.S. Federal Aviation Administration (FAA) Office of Aerospace Medicine through the National Air Transportation Center of Excellence for Research in the Intermodal Transport Environment at Purdue University under Cooperative Agreement 10-C-RITE-PU. Although FAA sponsored this project, it neither endorses nor rejects the findings of the research. This information is presented in the interest of invoking comments from the technical community about the results and conclusions of the research.

References

Bell, M.L., Peng, R.D., Dominici, F., 2006. The exposure–response curve for ozone and risk of mortality and the adequacy of current ozone regulations. Environmental Health Perspectives 114, 532-536.

Brohus, H., 1997. Personal exposure to contaminant sources in ventilated rooms. Ph.D. thesis, Aalborg University, Denmark.

Bhangar, S., Cowlin, S.C., Singer, B.C., Sextro, R.G., Nazaroff, W.W., 2008. Ozone levels in passenger cabins of commercial aircraft on North American and transoceanic routes. Environmental Science & Technology 42, 3938–3943.

Cano-Ruiz, J.A., Kong, D., Balas, R.B., Nazaroff, W.W., 1993. Removal of reactive gases at indoor surfaces: Combining mass transport and surface kinetics. Atmospheric Environment 27A, 2039–2050.

Coleman, B.K., Destaillats, H., Hodgson, A.T., Nazaroff, W.W., 2008. Ozone consumption and volatile byproduct formation from surface reactions with aircraft cabin materials and clothing fabrics. Atmospheric Environment 42, 642–654.

EPA (U.S. Environmental Protection Agency), 2006. Air quality criteria for ozone and related photochemical oxidants (final). U.S. Environmental Protection Agency, Washington, DC, EPA/600/R-05/004aF-cF.

FLUENT, 2009. ANSYS FLUENT 12.0 Theory Guide.

Lee, K., Vallarino, J., Dumyahn, T., Ozkaynak, H., Spengler, J.D., 1999. Ozone decay rates in residences. Journal of the Air & Waste Management Association 49, 1238-1244.

Liu, L.-J.S., Olson, M.P., Allen, G.A., Koutrakis, P., McDonnell, W.F., Gerrity, T.R., 1994. Evaluation of the harvard ozone passive sampler on human subjects indoors. Environmental Science & Technology 28, 915-923.

Morrison, G.C., Nazaroff, W.W., 2000. The rate of ozone uptake on carpets: Experimental studies. Environmental Science & Technology 34, 4963-4968.

NRC (National Research Council), 2002. The airliner cabin environment and the health of passengers and crew. National Academies Press.

Pandrangi, L.S., Morrison, G.C., 2008. Ozone interactions with human hair: Ozone uptake rates and product formation. Atmospheric Environment 42, 5079–5089.

Patankar, S.V., 1980. Numerical heat transfer and fluid flow. Taylor & Francis.

Rim, D., Novoselec, A., Morrison, G., 2009. The influence of chemical interactions at the human surface on breathing zone levels of reactants and products. Indoor Air 19, 324-334.

Russo, J., Khalifa, H.E., 2010. CFD analysis of personal ventilation with volumetric chemical reactions. HVAC&R Research 16, 799-812.

Russo, J., Khalifa, H.E., 2011. Surface reactions on the human body: Using personal ventilation to remove squalene oxidation products from the breathing zone with CFD. The 12th International Conference on Indoor Air Quality and Climate, Indoor Air Austin, TX, USA.

Sørensen, D.N., Weschler, C.J., 2002. Modeling-gas phase reactions in indoor environments using computational fluid dynamics. Atmospheric Environment 36, 9–18.

Spengler, J.D., Ludwig, S., Weker, R.A., 2004. Ozone exposures during trans-continental and trans-pacific flights. Indoor Air 14, 67–73.

Tamas, G., Weschler, C.J., Bako-Biro, Z., Wyon, D.P., Strom-Tejsen, P., 2006. Factors affecting ozone removal rates in a simulated aircraft cabin environment. Atmospheric Environment 40, 6122–6133.

Wang, H., Morrison, G., 2010. Ozone-surface reactions in five homes: Surface reaction probabilities, aldehyde yields, and trends. Indoor Air 20, 224-234.

Wang, H., Morrison, G.C., 2006. Ozone-initiated secondary emission rates of aldehydes from indoor surfaces in four homes. Environmental Science & Technology 40, 5263-5268.

Weschler, C.J., 2004. New directions: Ozone-initiated reaction products indoors may be more harmful than ozone itself. Atmospheric Environment 38, 5715-5716.

Weschler, C.J., 2006. Ozone's impact on public health: Contributions from indoor exposures to ozone and products of ozone-initiated chemistry. Environmental Health Perspectives 114, 1489-1496.

Weschler, C.J., Shields, H.C., 1999. Indoor ozone/terpene reactions as a source of indoor particles. Atmospheric Environment 33, 2301-2312.

Weschler, C.J., Shields, H.C., 2000. The influence of ventilation on reactions among indoor pollutants: Modeling and experimental observations. Indoor Air 10, 92–100.

Weschler, C.J., Wisthaler, A., Cowlin, S., Tamás, G., Strøm-Tejsen, P., Hodgson, A.T., Destaillats, H., Herrington, J., Zhang, J., Nazaroff, W.W., 2007. Ozone-initiated chemistry in an occupied simulated aircraft cabin. Environmental Science & Technology 41, 6177-6184.

Wisthaler, A., Tamás, G., Wyon, D.P., Strøm-Tejsen, P., Space, D., Beauchamp, J., Hansel, A., Märk, T.D., Weschler, C.J., 2005. Products of ozone-initiated chemistry in a simulated aircraft environment. Environmental Science & Technology 39, 4823-4832.

Wisthaler, A., Weschler, C.J., 2010. Reactions of ozone with human skin lipids: Sources of carbonyls, dicarbonyls, and hydroxycarbonyls in indoor air. Proceedings of the National Academy of Sciences 107, 6568.

Yakhot, V., Orszag, S.A., 1986. Renormalization group analysis of turbulence. Journal of Scientific Computing 1, 3-51.

Zhang, Z., Chen, X., Mazumdar, S., Zhang, T., Chen, Q., 2009. Experimental and numerical investigation of airflow and contaminant transport in an airliner cabin mockup. Building and Environment 44, 85–94.